Table 4.2.2.5. *Wavelengths of L-emission lines and L-absorption edges in Å (cont.)*

Z	Symbol	A	$L\alpha_2$	$L\alpha_1$	$L\beta_1$	$L\beta_2$	$L_{\rm I}$ abs. edge	$L_{\rm II}$ abs. edge	$L_{\rm III}$ abs. edge
83	Bi	209	*1.15540(14)*	*1.14390(13)*	*0.95205(11)*	*0.95526(18)*	*0.75649(58)*	*0.789102(88)*	*0.92387(11)*
			1.155377(15)	1.143877(30)	0.951992(13)	0.955194(59)	0.75711(15)	0.78871(15)	0.92341(15)
84	Po	209	*1.12549(13)*	*1.11393(12)*	*0.92228(10)*	*0.92932(18)*	*0.7332(13)*	*0.76325(13)*	*0.897554(85)*
			1.125497(74)	1.113877(59)	0.92201(30)	0.929384(74)			
85	At	210	*1.09670(13)*	*1.08510(12)*	*0.893639(96)*	*0.90444(17)*		*0.73868(13)*	
			1.096726(74)	1.085016(74)	0.89350(13)				
86	Rn	222	*1.06900(12)*	*1.05735(11)*	*0.866054(91)*	*0.88055(15)*		*0.71511(13)*	
			1.069006(74)	1.057246(74)	0.86606(13)				
87	Fr	223	*1.04232(11)*	*1.03063(11)*	*0.839482(86)*	*0.85751(15)*		*0.69240(13)*	*0.8251(27)*
			1.042316(74)	1.030505(74)	0.83941(13)	0.8580(30)			
88	Ra	226	*1.01662(11)*	*1.00489(10)*	*0.813866(82)*	*0.83533(16)*	*0.64449(15)*	*0.67077(12)*	*0.802768(44)*
			1.016575(74)	1.004745(74)	0.813762(74)	0.835383(74)	0.64451(15)	0.67071(15)	0.80281(15)
89	Ac	227	*0.99185(11)*	*0.980070(98)*	*0.789163(78)*	*0.81406(14)*		*0.64970(13)*	
			0.991795(74)	0.979945(74)	0.78904(13)				
90	Th	232	*0.96798(10)*	*0.956154(94)*	*0.765343(75)*	*0.79354(13)*	*0.60569(11)*	*0.62966(11)*	*0.760637(99)*
			0.9679082(23)	0.9560826(15)	0.7652610(14)	0.7935516(15)	0.60591(15)	0.62991(15)	0.76071(15)
91	Pa	231	*0.944896(96)*	*0.933002(90)*	*0.742301(71)*	*0.77321(12)*	*0.58759(12)*	*0.610354(92)*	*0.740958(97)*
			0.944834(74)	0.932854(74)	0.742331(74)	0.77371(15)			
92	U	238	*0.922622(93)*	*0.910674(86)*	*0.720056(68)*	*0.75462(12)*	*0.569885(39)*	*0.591930(66)*	*0.722319(52)*
			0.922572(13)	0.910653(13)	0.719995(12)	0.754692(13)	0.56951(15)	0.59191(15)	0.72231(15)
93	Np	237	*0.901230(88)*	*0.889223(83)*	*0.698624(65)*	*0.73623(11)*			
			0.901059(13)	0.889141(13)	0.698488(13)	0.736241(13)	0.55239(34)	0.57368(37)	0.704136(20)
94	Pu	244	*0.880355(85)*	*0.868290(79)*	*0.677776(60)*	*0.71848(11)*			
							0.53651(15)	0.55721(15)	0.68671(15)
95	Am	243	*0.860288(84)*	*0.848190(81)*	*0.657686(59)*	*0.70134(10)*			
96	Cm	248	*0.840918(80)*	*0.828776(78)*	*0.638265(56)*	*0.684815(98)*			
97	Bk	249	*0.822159(76)*	*0.809987(69)*	*0.619449(53)*	*0.668638(94)*			
							0.49060(49)	0.50851(52)	0.63748(98)
98	Cf	250	*0.803608(73)*	*0.791421(66)*	*0.601005(50)*	*0.652873(89)*			
							0.476569(92)	0.493804(98)	0.62300(19)
99	Es	251	*0.786043(70)*	*0.773837(63)*	*0.583354(49)*	*0.638227(82)*			
100	Fm	254	*0.769077(67)*	*0.756843(60)*	*0.566272(47)*	*0.623826(82)*			
			0.76904(62)	0.75674(60)	0.56619(34)	0.62369(41)	0.44966(13)	0.46534(12)	0.59414(20)

* These values are for the unresolved $L\beta_2$ and $L\beta_{15}$ emission lines.

4.2.2.12. *Structure and format of the summary tables*

Table 4.2.2.4 summarizes the theoretical and experimental results for prominent *K*-series lines and the *K*-absorption edge. For the emission lines, the upper number (in italics) is the theoretical estimate for this line and the lower number is the experimentally measured value (1) from Table 4.2.2.1 or (2) from the Bearden database or a reference that appeared after the Bearden database corrected to the optically based scale. For the *K* absorption edge, the upper number (also in italics) was obtained by combining emission lines and photoelectron spectroscopy (see Subsection 4.2.2.7), and the lower number is the experimentally measured value (1) from Table 4.2.2.3 or (2) from the Bearden database or a reference that appeared after the Bearden database corrected to an optically based scale. For the experimental emission and absorption entries, bold type is used for wavelengths directly measured on an optically based scale. The numerical values for wavelengths in angstrom units (1 Å = 0.1 nm) are given to a number of significant figures commensurate with their estimated uncertainties, which appear in parentheses after each theoretical and experimental value.

Figure 4.2.2.1 shows plots of the relative deviation between theoretical and experimental values for the *K*-series lines and the *K*-absorption edge as a function of *Z*. The error bars shown in the figure are the experimental uncertainties. In general, these plots show good agreement between theory and experiment except in the low-*Z* and high-*Z* regions. At the low-*Z* end of the table, the particular calculational approach used is not optimum, and the experimental data are suprisingly weak. At the high end, experimental data have rather large uncertainties, and thus do not provide an accurate test of the theory.

Table 4.2.2.5 summarizes the theoretical and experimental results for prominent *L*-series lines and the *L*-absorption edges. The experimental database of high-accuracy emission data is much more limited than was the case for the *K* series, and there have been very few high-accuracy edge-location measurements. The format of this table is similar to that of Table 4.2.2.4. For the emission lines, the upper number (in italics) is the theoretical estimate for this line, and the lower number is the experimentally measured value. Numbers in bold type were directly measured on the optical scale (see Table 4.2.2.2), and numbers in normal type are from the Bearden database or a reference that appeared after the Bearden database corrected to an optically based scale. For the *L*-absorption edges, the upper number (also in italics) is obtained by combining emission lines and photoelectron spectroscopy (see Subsection 4.2.2.7) and the lower number is the experimentally measured value. The numbers in bold type

Table 4.2.2.6. *Wavelength conversion factors*

Numbers in parentheses are standard uncertainties in the least-significant figures.

	Cu $K\alpha_1$	Mo $K\alpha_1$	W $K\alpha_1$
λ (Å)	1.54059292(45)	0.70931713(41)	0.20901313(18)
λ (Å*)	1.540562(3)	0.709300(1)	0.2090100
1 kxu	1.537400	0.707831	
Å*/Å	1.0000201(20)	1.0000242(22)	1.00001498(86)
kxu/Å	1.00207683(29)	1.00209955(58)	

are recent measurements by Kraft, Stümpel, Becker & Kuetgens (1996), and the numbers in normal type are from the Bearden database or a reference that appeared after the Bearden database corrected to an optically based scale. Figure 4.2.2.2 shows relative deviations between the theoretical and experimental values for most of the tabulated data. The error bars shown in the figure are the experimental uncertainties.

4.2.2.13. *Availability of a more complete X-ray wavelength table*

This article and the accompanying X-ray wavelength tables are an up-dated version of the contribution to the *International Tables for Crystallography*, Volume C, 2nd edition that was published in 1999. This article has been subject to more critical review and analysis and the data are consistent with the most recent adjustment of the fundamental physical constants (Mohr & Taylor, 2000). We believe that these data represent a significant improvement in consistency, coverage and accuracy over previously available resources. The results presented here are a subset of a larger effort that includes all *K*- and *L*-series lines connecting the $n = 1$ to $n = 4$ shells. The more complete table has been submitted for archival publication and will be made avaialble on the NIST Physical Reference Data web site. Electronic publishing of this resource will provide a convenient data resource to the scientific community that can be more easily up-dated and expanded.

4.2.2.14. *Connection with scales used in previous literature*

In order to compare historical data for X-ray spectra with the results in the present tabulation, certain conversion factors are needed. As discussed in the introduction, the principal units found in the literature are the xu and the Å* unit. There is the additional complication that there were several different definitions in use at various times and at the same time in different laboratories. For the convenience of the reader, we summarize in Table 4.2.2.6 the main conversion factors needed. The numerical values for the wavelengths in Å can be converted to energies in electron volts by using the conversion factor 12 398.41857 (49) eV Å (Mohr & Taylor, 2000).

Our current efforts owe their inception to the encouragement of the late A. J. C. Wilson, who persistently communicated the need for an updated wavelength resource for the crystallographic community. The larger effort evolved at NIST with the support of the Standard Reference Data Program as established with the help of the late Jean Gallagher, and sustained by the program's current Director, John Rumble. Early phases of the preparation of this material benefited from the efforts of John Schweppe. Cedric Powell supplied valuable advice in the area of electron binding energies. We are particularly grateful to the Editor, E. Prince, for his help and patience in the development of these wavelength tables. Richard Deslattes died between the first publication of this article and this revision. This work would not have been possible without his dedication to this project over more than a decade. The earlier wavelength table of the late J. A. Bearden, under whom one of the present authors (RDD) studied, was a significant influence on this project.

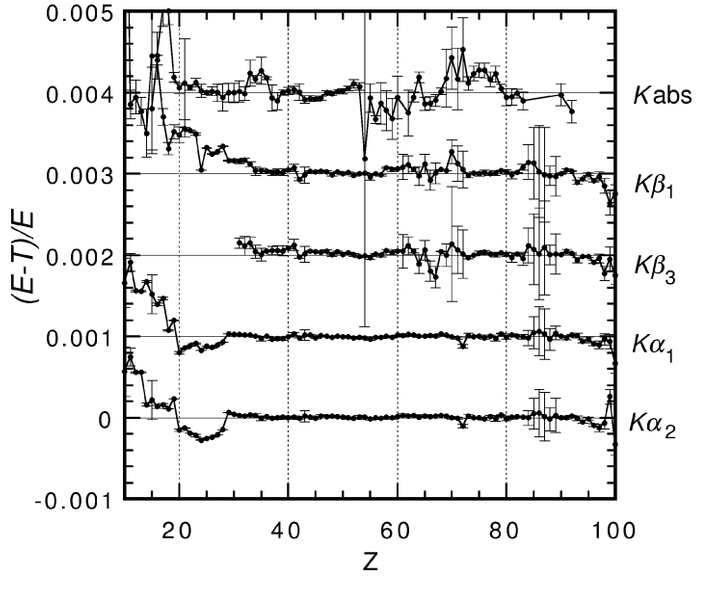

Fig. 4.2.2.1. Relative deviations between theoretical and experimental results for *K*-series spectra. The topmost data set concerns the *K*-edge location, while the other data sets, beginning at the bottom, refer to the $K\alpha_2$, $K\alpha_1$, $K\beta_3$ and $K\beta_1$, respectively. The ordinate scales have been displaced for clarity by the indicated multiples of 0.001.

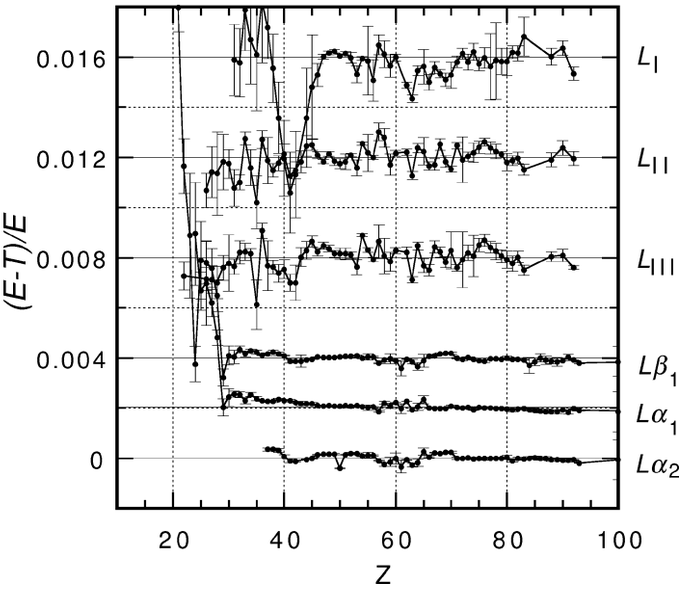

Fig. 4.2.2.2. Comparison of *L*-series data with experiment for the indicated range of *Z*. Indicated data, beginning at the bottom, refer to the $L\alpha_2$, $L\alpha_1$, and $L\beta_1$ emission lines and the L_{III}, L_{II}, and L_I absorption edges. For clarity, the plots have been displaced vertically by multiples of 0.002 for the emission lines and 0.004 for the absorption edges.